Oncogene (2006) 25, 3471–3478

www.nature.com/onc

ONCOGENOMICS

MAP1D, a novel methionine aminopeptidase family member is overexpressed in colon cancer

M Leszczyniecka[1,3], U Bhatia[1,4], M Cueto[1], NR Nirmala[1,3], H Towbin[2], A Vattay[1,3], B Wang[1], S Zabludoff[1,5] and PE Phillips[1]

[1]*Novartis Pharmaceuticals, East Hanover, NJ, USA and* [2]*Novartis Pharma AG, Basel, Switzerland*

N-terminal methionine removal is an important cellular process required for proper biological activity, subcellular localization, and eventual degradation of many proteins. The enzymes that catalyze this reaction are called Methionine Aminopeptidases (MAPs). To date, only two MAP family members, MAP1A and MAP2, have been well characterized and studied in mammals. In our studies, we have cloned a full length MAP1D gene. Expression and purification of full length recombinant protein shows that the sequence encodes an enzyme with MAP activity. MAP1D is overexpressed in colon cancer cell lines and in colon tumors as compared to matched normal tissue samples. Downregulation of MAP1D expression by shRNA in HCT-116 colon carcinoma cells reduces anchorage-independant growth in soft agar. These data suggest that MAP1D is a potentially oncogenic, novel member of the MAP gene family that may play an important role in colon tumorigenesis.
Oncogene (2006) **25,** 3471–3478. doi:10.1038/sj.onc.1209383; published online 27 March 2006

Keywords: methionine aminopeptidase; MAP1D; colon cancer; shRNA

Introduction

It is currently estimated that 60% of all proteins lose their initiator methionine after being synthesized (Meinnel *et al*., 1993; Giglione *et al*., 2000). This type of modification is critical for subsequent post-translational processes, such as N-terminal myristoylation and affects the activity of several important signal transduction proteins involved in growth control (Johnson *et al*., 1994). Methionine removal also affects the stability of selected proteins and targets them to the proteasome for subsequent degradation (Arfin and Bradshaw, 1988; Varshavsky, 1996).

N-terminal methionine removal is accomplished by a class of metalloenzymes called methionine aminopeptidases (MAPs) (Ben-Bassat *et al*., 1987; Miller *et al*., 1987; Chang *et al*., 1989; Chang *et al*., 1990). This process depends on the context of the initiator methionine and the second residue; the methionine is removed only when the second residue in the peptide sequence is small and uncharged (Flinta *et al*., 1986). Diversity of MAP enzymes varies among all organisms. While there is only one MAP in prokaryotes, most eukaryotes have two types of MAP enzymes, MAP1 and MAP2 (Chang *et al*., 1989; Arfin *et al*., 1995; Li and Chang, 1995). *Arabidopsis thaliana* is the exception since six MAPs have been identified (Giglione *et al*., 2000).

The understanding of MAP function primarily comes from the work on model organisms, especially bacteria and yeast. MAP function in bacteria is essential since deletion of the gene encoding MAP protein is lethal (Chang *et al*., 1989). In *Saccharomyces cerevisiae,* two MAP genes have been identified (Chang *et al*., 1989; Li and Chang, 1995). Studies show that MAP1 has a much more general and essential function since the deletion of the *map1* gene results in more severe growth inhibition than the deletion of the *map2* gene (Chen *et al*., 2002). The differential effects of gene loss have been suggested to be a consequence of isoform-specific substrate processing, since MAP1 and MAP2 exhibit different cleavage efficiencies against synthetic peptides (Chen *et al*., 2002). In plants, a large number of MAP isoforms has been suggested to reflect differential targeting to specific subcellular compartments (Giglione *et al*., 2000).

In mammals, the role of MAPs has been defined largely through the use of MAP inhibitors. Fumagillin, TNP-470, and ovalicin are MAP2 specific inhibitors. These compounds are also selective inhibitors of endothelial proliferation, suggesting a role for MAP2 in tumor angiogenesis and metastasis (Sing *et al*., 1997; Lowther and Matthews, 2000). Besides the antiangiogenic effect of the MAP2 inhibitors, initial epidemiology studies suggest that MAP2 is highly expressed in mesothelioma and B-cell lymphoma (Catalano *et al*., 2001; Kanno *et al*., 2002). MAP2 also has been reported to interact with a metastasis associated protein, S100A4 (Endo *et al*., 2002). In addition, transfection of

Correspondence: Dr M Leszczyniecka, Novartis Institutes for Biomedical Research, Cambridge, MA 02139, USA.
E-mail: magdalena.leszczyniecka@novartis.com
[3]Current address: Novartis Institutes for Biomedical Research, Cambridge, MA 02139, USA
[4]Current address: Omni Genetics, Menlo Park, CA 94025, USA
[5]Current address: AstraZeneca Pharmaceuticals LP, Waltham, MA 02451, USA
Received 8 July 2005; revised 21 November 2005; accepted 25 November 2005; published online 27 March 2006

mesothelioma cells with antisense oligonucleotides to MAP2 reduced the growth potential of these cells (Catalano *et al*., 2001).

Although MAP1A exhibits significant homology to MAP2, fumagillin and its derivatives do not inhibit MAP1A (Sing *et al*., 1997; Lowther and Matthews, 2000). Just recently, a novel bengamide analog, LAF389, has been shown to inhibit both MAP1A and MAP2 proteins (Towbin *et al*., 2003). LAF389 inhibits both endothelial and tumor epithelial cell growth *in vitro*, and causes tumor growth inhibition and regression *in vivo* (Kinder *et al*., 2001; Towbin *et al*., 2003). Given that N-terminal processing has become the target for new drugs, a better characterization of this process in higher eukaryotes is required.

This report describes cloning and initial characterization of a full length MAP1D, a MAP that is closely related to MAP1A. In our studies, we have found that MAP1D expression is elevated in colon cancer cell lines and in samples from colon cancer patients. Furthermore, we have found that downregulation of MAP1D expression by shRNA in HCT-116 colon carcinoma results in the reduced potential of these cells to form colonies in soft agar. These data suggest that MAP1D may potentially represent a novel oncogene, with a role in colon tumor growth.

Results

A search of the GenBank database with the MAP1A and MAP2 protein sequences lead us to believe that additional MAPs may be present in the human genome. A tBLASTn search of a GENBANK database (http://www.ncbi.nlm.nih.gov/BLAST/) with the MAP1A protein sequence lead to the identification of an additional MAP like sequence that was designated as MAP1D based on the sequence alignment and domain analysis (Serero *et al*., 2003; Addlagatta *et al*., 2005) (Genbank #BC029123). The cDNA fragment (~1700 bp) (Figure 1a, red box), when translated, exhibited high homology to MAP1A. Analysis of the MAP1D genomic region identified an additional contiguous open reading frame extending to an ATG start codon located 487 bp upstream of the sequence reported in GenBank (Figure 1a). The complete ORF was cloned from fetal brain poly(A) RNA using RT–PCR as described in the materials and methods section (Genbank #DQ05576). In order to demonstrate that the additional ORF was transcribed, probes from the additional 5′ sequence and the original sequence were hybridized to poly(A) RNA from fetal brain (Figure 1b). Both probes hybridized to the same band, confirming that the upstream region is a part of MAP1D cDNA (Figure 1b). Translation of this cDNA indicated that MAP1D encodes a putative protein of 51 kD with a domain structure typical of the M24 metalloprotease family. Analysis of the MAP1D amino-acid sequence with the prosite sequence analysis tool showed that residues 391–412 contained the MAP subfamily 1 signature (Figure 1c black box). Residues 216–455 showed a peptidase M24 signature, which forms part of the metal-binding site (Figure 1c, red underline). Analysis of the alignment between MAP1A, MAP2, and MAP1D showed that MAP1D is more closely related to MAP1A (49%) than to MAP2 (16%) over the entire protein sequence (Figure 1c). The homology of MAP1D to MAP2 (16%) was lower than that of MAP1A to MAP2 (22%). Furthermore, we collected sequence information for all of the known members of this MAP family using the BLAST search of nr database (http://www.ncbi.nlm.nih.gov/BLAST/). Alignment was carried out using ClustalW followed by a phylogenetic analysis using Neighbor Joining (NJ) method. This analysis revealed that additional members of the MAP1D family are present in mouse, fly and plants and showed that this protein belongs to MAP1D subfamily of enzymes (Figure 1d) (Serero *et al*., 2003; Addlagatta *et al*., 2005). Phylogenetic analysis showed that MAP1D and MAP1A families are closely related and may encode enzymes with similar properties but different localization (Serero *et al*., 2003). Based on the alignment and the domain analysis, the identified cDNA, MAP1D, encodes a new member of human MAP family and belongs to Type I MAP subfamily.

Since the MAP1D sequence exhibited homology to the family of MAPs, it became critical to demonstrate the MAP enzymatic activity of MAP1D. To facilitate these studies, GST fusion constructs of MAP1A, 2, and MAP1D were purified as described in materials and methods. The purity and quantity of all three purified MAP proteins was estimated by Coomasie staining (Figure 2a). A colorimetric assay was developed to test for MAP activity (Towbin *et al*., 2003). In this assay, we found that at similar protein concentrations, MAP1A was most efficient in removing methionine from Met-Ala-Ser (MAS) peptide substrate (Figure 2b). As compared to MAP1A and MAP2, MAP1D was the least efficient in removing the methionine from Met–Ala–Ser substrate (Figure 2b). No activity was seen with any of the MAP isoforms using Glu–Ala–Ser and Leu–Ala–Ser peptides as substrates (data not shown).

Since previous reports suggested MAPs were overexpressed in various cancers (Catalano *et al*., 2001; Kanno *et al*., 2002), it was of interest to establish whether MAP1D expression was also upregulated in cancer cells. Using quantitative real-time RT–PCR, we found that MAP1D expression was lowest in normal HUVEC and HMVEC, somewhat higher in WI38 fibroblasts and A549 lung carcinoma cells, and highest in H1299 and HCT-116 cells (Figure 3a). MAP2 expression was the highest in HCT-116 and elevated in WI-38, A459, and H1299 cells. (Figure 3a). MAP1A expression was slightly elevated in all of tested cancer cell lines compared to HUVEC and HMVEC (Figure 3a).

To determine whether this finding was also observed in human tumor samples, total RNA was isolated from matched normal and tumor tissue. In lung and kidney no difference in expression was observed in MAP isoforms between tumor and matched normal samples (data not shown). For MAP1A and MAP2 isoforms, mRNA expression levels were also the same in colon tumor versus matched normal tissue. In contrast, the mRNA

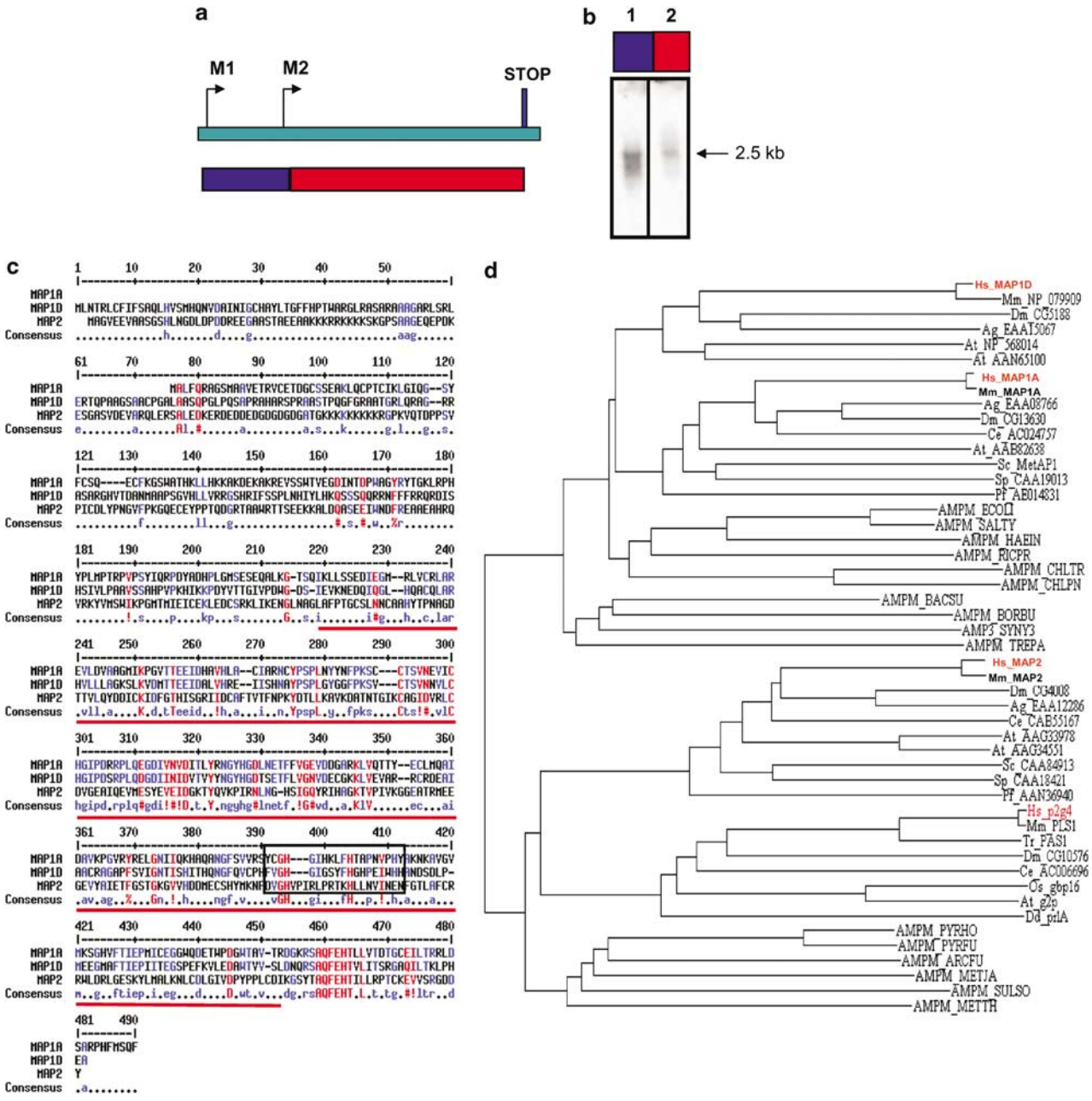

Figure 1 (**a**) Graphic representation of the MAP1D cDNA showing two (M) methionines that could serve as an initiator methionines. M2 represents the methionine previously described as the initiator methionine (25). M1 represents the full length initiator methionine for MAP1D. (**b**) Northern blot hybridized with the previously identified MAP1D cDNA (blue box) and 5′ extended MAP cDNA (red box). (**c**) Alignment of the three MAP family members, MAP1A, MAP2, and MAP1D. Alignment of MAP1A, 2, and 1D was performed using MultAlin (http://prodes.toulouse.inra.fr/multalin/multalin.html) (Corpet, 1988). A residue that is highly conserved appears in high-consensus color (90%, red) and as an uppercase letter in the consensus line. A residue that is weakly conserved appears in low-consensus color (50%, blue) and as a lowercase letter in the consensus line. Other residues appear in black. A position with no conserved residue is represented by a dot in the consensus line. !, IV; $, LM; %, FY; #, NDQE . Black box (378–396AA) – MAP subfamily 1 signature. Red underlined region (216–455 AA) – peptidase M24 signature (**d**) (**b**) Phylogenetic tree of a selected members of MAP family. For a complete description of the method of tree construction, see material and methods. The known family members are represented by their names. The uncharacterized proteins are represented by the species name followed by their accession numbers. Ag *(Anopheles gambiae)*, At *(Arabodopsis thaliana)*, Ce (*Caenorhabditis elegans)*, Dd *(Dictyostelium discoideum)*, Dp *(Drosophila melanogaster)*, Hs *(Homo sapiens)*, Mm *(Mus musculus)*, Sc *(Saccharomyces cerevisiae)*, Sp *(Schizosaccormyces pombe)*, Pf (*Plasmodium falciparum)*, Tr *(Takifugu rubripes)*, Os *(Oryza sativa)*, AMPM_CHLPN *(Chlamydophila pneumoniae)*, AMPM_CHLTR *(Chlamydia trachomatis)*, AMPM_BORBU *(Borrelia burgdorferi)*, AMPM_TREPA *(Treponema pallidum)*, AMPM_ECOLI *(Escherichia coli)*, AMPM_BACSU *(Bacillus subtilis)*, AMPM_SYN *(Synechocystis* sp., AMPM_HAEIN (*Haemophilus influenzae*), AMPM_PYRHO (*Pyrococcus horikoshii*), AMPM_PYRFU (*Pyrococcus furiosus*) AMPM_ARCFU (*Archeoglobus fulgidus*), AMPM_METJA (*Methanococcus jannaschii.*), AMPM_SULSO (*Sulfolobus solfataricus.*), AMPM_METTH (*Methanobacterium thermoautotrophicum)*, AMPM_TREPA *(Treponema pallidum)*, *AMPM_BORBU (Borrelia burgdorferi)*, AMPM_SALTY *(Salmonella typhimurium.*), AMPM_RICPR (*Rickettsia prowazekii)*.

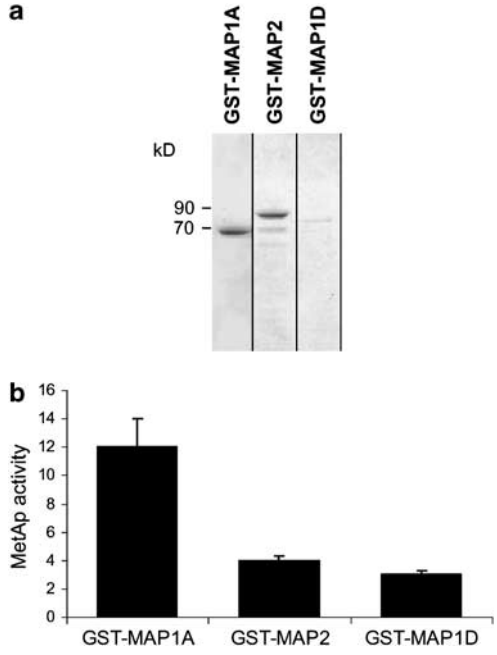

Figure 2 MAP purification and activity (**a**) Coomasie staining of GST-MAP1A, GST-MAP2, and GST-MAP1D (**b**) *In vitro* MAP activity of GST-MAP1A, GST-MAP2, and GST-MAP1D. The fold activation represents the enzyme activity over the activity observed in a reaction without the enzyme.

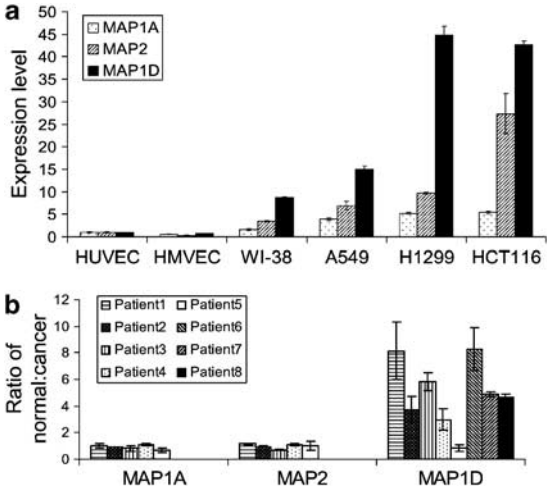

Figure 3 Profile of MAP mRNA expression in various cell lines (**a**) or in colon tumors from patients (**b**). (**a**) Expression of MAP1A, MAP2, and MAP1D was examined in normal (HUMEC, HMVEC) and transformed cells (WI-38, A549, H1299, HCT116) by quantitative RT–PCR as described in the materials and methods section. All values were first normalized to the GAPDH levels and then expressed as the fold upregulation of the gene expression found in the specific cancer cell lines over the levels found in HUVEC cells. (**b**) MAP1A, MAP2, MAP1D expression was examined by real time PCR in colon tumors and normal matched tissue controls from patients. The graph shows fold upregulation of MAP expression in tumor versus normal samples.

expression of MAP1D was significantly upregulated in colon tumors from four out of five patients (Figure 3b).

To determine whether the mRNA upregulation was accompanied with an increase in protein expression,

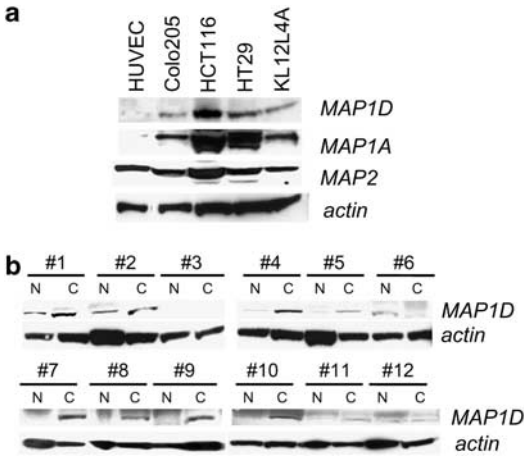

Figure 4 Expression of MAP1D protein in (**a**) various cell lines and (**b**) in patient samples. The expression was detected by Western blotting as described in the material and methods with the rabbit anti-MAP1D antibody (1:500), followed by goat anti-rabbit-HRP secondary antibody (1:2000), and developed with ECL reagents (Amersham Pharmacia, Piscataway, NJ). Actin staining was done for normalization purposes with goat-anti-actin antibody (1:1000) followed by incubation with secondary rabbit anti-goat (1:2000) antibody.

antibodies to MAP1D were made as described in the materials and methods section. Since the previous results suggested that MAP1D expression was elevated only in colon cancers, we compared the expression levels of all three MAP isoforms in four colon carcinoma cell lines (Colo205, HCT116, HT29, KL12L4A) to the levels found in normal HUVEC cells. Western blot analysis with the MAP1D specific antibody yielded the expected 50 kDa band. We found that MAP1D protein expression was increased in all four colon lines compared to HUVEC, with the highest expression levels found in HCT-116 and HT-29 cells (Figure 4a). MAP1A protein expression also was elevated in the four colon lines compared to HUVEC, with the highest levels found in the HCT-116 cells (Figure 4a). MAP2 expression was roughly comparable in the colon lines versus HUVEC (Figure 4a). MAP1D protein expression was also measured in matched pairs of human colon tumor and normal tissue. Of the 12 patient samples tested, the expression of MAP1D was not detectable in one sample. MAP1D expression was increased in eight of 12 tumor samples compared to matched normal tissue; no difference in expression was observed in three out of 12 tumor and normal pairs. Interestingly, while the expression of MAP1A was observed to be elevated in colon cancer cell lines, MAP1A expression was not higher in colon tumor samples (data not shown). These data suggest that MAP1D expression, but not MAP1A or MAP2, may be a common observation in colon cancer.

Since HCT-116 colon carcinoma cells expressed the highest levels of MAP1D, we tested the growth dependence of these cells on MAP1D expression. To perform these experiments, a plasmid was constructed with an shRNA to MAP1D. A plasmid containing the mismatch shRNA was used as a control. The constructs

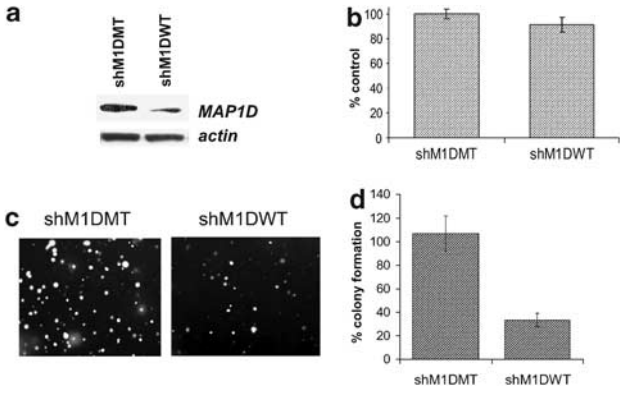

Figure 5 Downregulation of MAP1D expression with shRNA against MAP1D (**a**) Western blot with the rabbit anti-MAP1D antibody (1:500), followed by goat anti-rabbit-HRP secondary antibody (1:2000), and developed with ECL reagents (Amersham Pharmacia, Piscataway, NJ) (see material and methods section for complete description). Actin staining was done for normalization purposes with goat-anti-actin antibody (1:1000) followed by the incubation with secondary rabbit anti-goat (1:2000) antibody. (**b**) colony formation assay of MAP1D shRNA transfected HCT-116 and mismatch transfected HCT-116 cells. For complete description see materials and methods. Data shown are from a representative experiment repeated four times in triplicate. (**c**) MTS proliferation assay. shM1DWT HCT-116, cells stably transfected with wild type shRNA to MAP1D. shM1DMT-HCT-116, cells stably transfected with mismatch shRNA to MAP1D. To calculate difference in proliferation and cell numbers, all measurements were normalized to the control (shM1DMT transfected HCT-116) which was set as 100%. (**d**) Quantitation of the colony formation assay. MAP1D shRNA transfected HCT-116, HCT-116 cells stably transfected with wild type shRNA to MAP1D. Mismatch HCT-116, HCT-116 cells stably transfected with mismatch shRNA to MAP1D. To calculate difference in colony number, all measurements were normalized to the control (shM1DMT transfected HCT-116 cells).

were transfected into HCT-116 cells and selected with zeocin. Following antibiotic selection, MAP1D levels were measured by Western blotting. MAP1D expression was reduced by about 60% in MAP1D shRNA transfected HCT-116 cells as compared to the mismatch shMAP1D transfected HCT-116 cells (Figure 5a). We did not observe any difference in proliferation, cell survival, or cell numbers between the MAP1D shRNA transfected HCT-116 cells and the mismatch control transfected HCT-116 cells as assessed by an MTS assay (Figure 5b). In contrast, a major difference was observed in growth in soft agar, an assay that measures the requirement for cell attachment to a solid substratum, reflecting changes in adhesion properties of the cells. Mismatch-transfected HCT-116 cells showed rapid growth and colony formation, whereas the MAP1D shRNA-transfected HCT-116 cells exhibited a dramatically reduced potential to form colonies in soft agar (Figure 5b and c).

Discussion

Removal of the N-terminal methionine is an important cellular process carried out by a family of proteins known as MAPs. This cellular process is essential for cell survival since cells die in the absence of MAP enzymes (Chang *et al*., 1989, 1990; Meinnel *et al*., 1993). To date, only two MAP enzymes, MAP1A and MAP2, have been thoroughly studied in mammalian cells (Bradshaw and Yi, 2002). Here, we describe the full length cloning and characterization of another member of the MAP family, MAP1D, which belongs to the Type 1 MAP enzymes (Figure 1c).

The existence of multiple MAP isoforms might in part reflect differential subcellular localizations and function (Giglione *et al*., 2003). Phylogenetic analysis (Figure 1d) of the human MAP isoforms suggests that human MAP1D pairs with the mitochondrial MAP orthologs previously identified in plants (Giglione *et al*., 2003). This analysis is consistent with a recent report describing the presence of human orthologs of the bacterial N-terminal methionine excision pathway in mitochondria (Serero *et al*., 2003). Although the importance of N-terminal methionine removal in organelles is still not clear, evidence from plant studies suggests that this process may affect the stability of specific organellar proteins (Cutforth and Gaul, 1999; Giglione and Meinnel, 2001; Serero *et al*., 2001).

MAP1A and MAP2 proteins exhibit similar substrate specificity when tested *in vitro* (Arfin *et al*., 1995, Lowther and Matthews, 2000; Chen *et al*., 2002). In our studies, we have compared the ability of all three MAP isoforms to remove the methionine from a methionine–alanine–serine peptide (Figure 2). We found that MAP1D was least efficient in removing the methionine from the MAS substrate as compared to MAP1A and MAP2 (Figure 2). The limited enzymatic activity of MAP1D may reflect a preference for alternative amino-acid residues in the positions proximal to the methionine. Alternatively, MAP1D activity may be enhanced by different metal cofactors, as has recently been suggested for other MAP family members (Garrabrant *et al*., 2004).

MAP activity has been suggested to be important for tumor growth. The MAP2 inhibitors fumagillin, TNP-470, and ovalicin have been shown to exhibit a very potent antiproliferative effect on endothelial cells, suggesting that MAP2 may contribute to tumor angiogenesis and cancer metastasis (Sing *et al*., 1997; Lowther and Matthews, 2000). More recently, LAF389, a synthetic analog of bengamides, a family of marine natural products, has been shown to inhibit both MAP1A and MAP2 proteins, and to have potent antiproliferative activity *in vitro* and *in vivo* (Kanno *et al*., 2002). Expression analysis data suggests that MAPs are overexpressed in some cancers (Catalano *et al*., 2001; Kanno *et al*., 2002). We found that while the expression of all MAP family members was elevated at the mRNA level in colon cancer cell lines as compared to HUVEC and HMVEC controls, only MAP1A and MAP1D showed the same pattern at the protein level (Figures 3 and 4). When protein expression was analysed in tumor samples, overexpression was detected of MAP1D, but not of MAP1A or MAP2. Overexpression of MAP1D protein was found nine of 12

colon tumors; no changes in MAP1D expression were found in lung and kidney tumors (data not shown) (Figures 3 and 4). Collectively, the expression analysis data suggested that MAP1D may be important for colon cancer growth.

Since MAP1D expression analysis has shown that this gene was overexpressed in colon tumors, we have examined the effects of suppressing MAP1D expression on the growth of HCT-116 colon carcinoma cells. Downregulation of MAP1D expression by shRNA did not change the growth properties such as proliferation or cell survival of HCT-116 cells in monolayer cell culture conditions (Figure 5b), but it was able to reduce anchorage independant growth of these cells suggesting that MAP1D may affect various properties of cancer cells including adhesion (Figure 5c and d). This effect on anchorage-independent growth was not seen in cells with low endogenous levels of MAP1D protein; transfection of MAP1D shRNA and the mismatch control into A549 lung carcinoma cells had no effect on growth in either monolayer or anchorage independent conditions (data not shown). These data collectively suggest that MAP1D may be an important factor regulating growth in colon tumors.

In summary, we have identified and characterized MAP1D, a novel member of the MAP family. We have found that MAP1D is overexpressed in colon cancer cell lines and in colon tumors. Overexpression of MAP1D may be important in tumorigenesis, since shRNA reduction of MAP1D in an overexpressing cell line resulted in a decreased potential of these cells to grow in soft agar. These data collectively suggest that MAP1D may be an attractive target for chemotherapy in colon carcinoma.

Materials and methods

Cell culture, MTS and soft agar assay

Colon carcinoma (HCT-116, HT29, Colo205, KM12L4A), human small cell lung carcinoma (H1299), non-small cell lung carcinoma cells (A549), and T-antigen transformed fibroblasts (WI38) were purchased from ATCC and cultured in RPMI media supplemented with 10% FBS and 1% penicillin/streptomycin. Human umbilical vein endothelial cells (HUVEC) and human microvessel endothelial cells (HMVEC) were grown according to manufacturer's suggestions (Clonetics, Walkersville, MD). All cells were grown at 37°C in a 5% CO_2/95% air humidified incubator. Sf9 cells were grown in suspension in Sf-900 II SFM media supplemented with 10% FBS and 1% penicillin/streptomycin at 27°C. For the MTS assay we used the CellTiter 96® AQ_{ueous} One Solution Cell Proliferation Assay (Promega, Madison, WI). Cells were seeded at 2×10^3/well in a 96-well plate in triplicates. On day 5, 10 μl of MTS reagent was added to 100 μl of media. The color was allowed to develop for 4 h. Absorbance was measured using SpectraMax reader at 490 nM. For soft agar assays, 5×10^3 HCT116 cells were suspended in top agar (0.35% bacto-agar, 10% FBS, 1% penicillin/streptomycin in RPMI 1640) over a 0.8% base agar (10% FBS, 1% penicillin/streptomycin in RPMI 1640). The plates were maintained at 37°C and 5% CO_2. After 3 weeks the number of colonies was counted.

Cloning of full length MAP1D

MAP1D was identified by database mining, using a BLAST search with the protein sequence of MAP1A, of the SWISS-PROT database (http://www.ncbi.nlm.nih.gov/BLAST). This analysis led to the identification of a MAP like sequence of 1700 bp, previously deposited in the Genbank (Accession #BC029123). Analysis of the genomic region containing the MAP1D EST sequence identified an upstream ATG codon that was not present in the original EST sequence. MAP1D was cloned from poly (A) fetal brain RNA (Clontech, Palo Alto, CA) (Table 1) using the Advantage™ RT-for-PCR kit according to the manufacturer's protocol (Clontech, Palo Alto, CA). Two rounds of PCR reactions were performed to obtain the full length MAP1D cDNA. The conditions were 95°C for 1 min, 34 cycles of 95°C for 1 min, and 68°C for 3 min, followed by 10 min at 68°C. The primers P1 and P2 which were designed in the 5′ and 3′ region of MAP1D gene were used for the first reaction, while the nested primers P3 and P4 were used for the second reaction (Table 1). P3 and P4 primers contained ends compatible with the pDON201 cloning vector (Invitrogen, Carlsbad, CA) subsequently used to produce the GST tagged MAP1D baculovirus.

Alignments and phylogenetic analysis

Alignment of MAP1A, MAP2, and MAP1D was done using ClustalW (Higgins *et al*., 1996). The tree was constructed with Neighbor Joining (NJ) using the NJ Plot method based on a distance matrix derived from the multiple sequence alignment.

RNA extraction and real-time PCR

Total RNA was extracted from cells using an RNeasy kit according to the manufacturer's suggestions (Ambion, Austin, TX). cDNA was synthesized from total RNA (2 μg) using a Taqman kit (Roche, Indianapolis, IN), random hexamers, and MMLV reverse transcriptase. Of the resulting cDNAs 5 μl of 100 μl were used as templates for quantitative real time PCR. Quantitative PCR was performed using a SYBR® Green PCR kit (Perkin Elmer, Wellesley, MA) with GeneAmp7500 Sequence Detection system (Perkin Elmer, Wellesley, MA) at

Table 1 PCR primers for cloning

Primer name	*Sequence*
P1	5′-tgctatgttgaaccactagattgtgct-3′
P2	5′-gtcgcggtgacctggtgcctttt-3′
P3	5′-ggggacaagtttgtacaaaaaagcaggcttgaacactagatt-3′
P4	5′-ggggaccactttgtacaagaaagctgggtctcaggcctcatggggtag-3′
P5	5′-gtggcgtccacctgctcgtc-3′
P6	5′-tcggtcacgtggccgcgag-3′
M1DWT-S	5′-tcgagaaaaaaatggctaccatggagacacctctcttgaaggtgtcc tccat ggtagccattgggaa-3′
M1DWT-AS	5′-agctttcccaatggctaccatggagacaccttcaagagaggtgtctc catggtagccatttttttc-3′
M1DMT-AS	5′-tcgagaaaaaaaatggctatcgcggagacacctctcttgaaggtgtc tccgcgatagccattgggaa-3′
M1DMT-S	5′-agctttcccaatggctatcgcggagacaccttcaagagaggtgtctc cgcgatagccatttttttc-′3
GAPDH-S	5′-gaaggtgaaggtcggagtca-3′
GAPDH-AS	5′-gaagatggtgatgggatttc-3′
M1D-S	5′-gcatcatgcaaacgacagtga-3′
M1D-AS	5′-gatccctccgtgatgattgg-3′
MAP1A-S	5′-ggggacaagtttgtacaaaaaagcaggcttaatggcggccgtgga gacgcg-3′
MAP1A-AS	5′-ggggaccactttgtacaagaaagctgggtcttaaaattgagacat gaagtg-3′
MAP2-S	5′-tccctcgtctctctcctcgggcaacatggc-3′
MAP2-AS	5′-catgctcgagttaatagtcatctcctctt-3′

95°C for 1 min, and 40 cycles of 95°C at 30 s and 60°C for 1 min using M1D-S and M1D-AS primers to amplify MAP1D and GAPDH-S and GAPDH-AS to amplify GAPDH (Table 1). For each of the assays, a standard curve for MAP1A, MAP2 or MAP1D was prepared using serial dilutions of cDNA. The fluorescence of the reporter dye was plotted against the number of cycles. The threshold cycle was calculated as the cycle number at which the fluorescence of the reporter dye crossed the threshold in the log linear range of PCR. Copy numbers of the respective MAP1A, MAP2, MAP1D or GAPDH genes were quantified by interpolating the results from the threshold cycles. All gene levels were then normalized to the GAPDH levels in each tested sample. Subsequently for the analysis of the patient samples, the level of a given gene in the cancer sample was divided by the level of that gene in the normal sample to obtain the percent upregulation in cancer versus normal. Each of the experiments was performed in triplicate.

Northern blots
Poly(A) RNA (2 μg) from Fetal Brain (Clontech) was resolved in 1% agarose gel with 2% formaldehyde and then transferred to nylon membrane (Hybond-N). Probes for hybridization were prepared by PCR amplification of the boxed regions indicated in Figure 1. The 1.7 kb cDNA sequence corresponding to Genbank Accession # BC029123 was PCR amplified using primers P5 and P2 (Figure 1a, blue box). The additional 0.4 kb fragment of open reading frame 5′ to the 1.7 kbase sequence was PCR amplified using primers P1 and P6 (Figure 1a red box). PCR amplified fragments were then labeled with [α-^{32}P]dCTP according to the manufacturers suggestions (Roche, Basel). The membrane was hybridized with both of the ^{32}P-labeleled cDNA probes and then exposed for autoradiography.

Patients samples
Matched tumor and normal tissue specimens were obtained from NDRI, Philadelphia, PA. The samples were homogenized with a Polytron PT 1200. Protein lysates were prepared in triple detergent buffer (50 mM Tris-Cl pH 8, 150 mM NaCl, 0.1% SDS, 1% Nonidet P-40, 0.5% Sodium Deoxycholate) containing Complete Mini Protease Inhibitor (Roche, Indianapolis, IN).

Preparation of MAP1D antibody
A polyclonal rabbit antiserum against the synthetic peptide HANDSDLPMEEGC (conjugated to KLH using m-maleimidobenzoyl-*N*-hydroxysuccinimide ester chemistry) was custom-produced by Neosystem Laboratories (Strasbourg, France). The serum was filtered and loaded on an affinity column (SulfoLink, Pierce, Rockford, Il) of the same peptide. Antibodies were eluted with 0.1 M glycine, 0.1 M NaCl, pH 2.5.

Western blotting
Total protein (50 μg) was resolved on 10% Bis-Tris gels in 1 × MOPS buffer and transferred to nitrocellulose membranes in 1 × transfer buffer (Invitrogen, Carlsbad, CA). Blots were blocked in 5% milk, followed by subsequent incubation with primary and secondary antibodies as described in the figure legends, and detected using ECL (Amersham Pharmacia, Piscataway, NJ).

Construction of GST-tagged expression plasmids carrying MAP 1A, 2, and 1D cDNAs
MAP1A and MAP2 genes were obtained by PCR from a human fetal brain cDNA library (Clontech, Palo Alto, CA) using Pfx DNA polymerase (Invitrogen, Carlsbad, CA) with the following conditions: 95°C for 1 min, and 34 cycles of 95°C for 1 min, 55°C for 1 min and 72°C for 1 min with the following primers: MAP1A-S and MAP1A-AS for MAP1A; MAP2-S and MAP2-AS for MAP2 (Table 1). MAP1D was obtained as described in the cloning of MAP1D section. All PCR products were then inserted into pDONR201 vector (Invitrogen, Carlsbad, CA). Following sequence confirmation, MAP1A, MAP2, and MAP1D were then transferred to pDEST20, a GST fusion, baculovirus expression vector. The baculovirus DNA containing all genes of interest was then made and used to transfect Sf9 insect cells using Cellfectin reagent (Invitrogen, Carlsbad, CA).

Purification of MAPs
GST-MAP1A, 1D, and 2 were purified from Sf21 insect cells using glutathione (GSH) agarose (Amersham Pharmacia, Piscataway, NJ). The cell pellet was lysed in Buffer I (25 mM HEPES, pH 7.5, 100 mM KCl, 1.5 mM $MgCl_2$, 1% NP-40, 0.1 mg/ml pefabloc, 2 μg/ml leupeptin, 1 μg/ml pepstatin, 2 μg/ml aprotinin), bound to GSH agarose, washed with Buffer I and eluted with Buffer II (25 mM HEPES, pH 7.4, 100 mM KCl, 1.5 mM $MgCl_2$, 50 mM GSH). The sample was dialyzed in Buffer III (25 mM HEPES, pH 7.4, 100 mM KCl, 1.5 mM $MgCl_2$) to remove the GSH. The proteins were quantitated using a standard Coomasie staining protocol.

MAP assay
The reaction was carried out in MAP assay buffer (20 mM HEPES, pH 7.5, 40 mM KCl, 1 mM $CoCl_2$) in the presence of Methionine-Alanine-Serine (MAS) peptide substrate (Bachem) for 30 min at 37°C. The reaction was stopped and developed with stop buffer (1% ninhydrin, 12.5% Acetic acid, 1.25 mM $CdCl_2$) for 1 h at 37°C and measured at 490 nm.

Construction of shRNA constructs and cell transfection
Wild type (M1DWT-S and M1DWT-AS) and control oligonucleotide (M1DMT-S and M1DMT-AS) in sense and antisense orientation containing MAP1D sequence and *Hind*III and *Xho*I overhangs were first phosphorylated using T4 kinase (Roche, Indianapolis, IN) according to the manufacturer's suggestions and annealed to each other. The double-stranded oligonucleotides were then ligated into the *Hind*III/*Xho*I site in the pBH1 vector (pBluscriptSK(+) based vector containing H1 promoter cloned in the *Bam*HI/*Hind*III sites. To allow selection, the ZEO cassette was inserted into the pBH1 vector. Stable cell lines expressing either wild-type MAP1D shRNA or the mismatch MAP1D shRNA were constructed in HCT-116 by transfection of the pBH1 plasmid containing either wild type MAP1D or mismatch shRNA with Lipofectamine 2000 (Invitrogen, Carlsbad, CA) then selected with Zeocin (Invitrogen, Carlsbad, CA) for 3 weeks.

References

Addlagatta A, Quillin ML, Omotoso O, Liu JO, Matthews BW. (2005). *Biochemistry* **44**: 7166–7174.
Arfin SM, Bradshaw RA. (1988). *Biochemistry* **27**: 7979–7984.
Arfin SM, Kendall RL, Hall L, Weaver LH, Stewart AE, Matthews BW *et al*. (1995). *Proc Natl Acad Sci USA* **92**: 7714–7718.

Ben-Bassat A, Bauer K, Chang SY, Myambo K, Boosman A, Chang S. (1987). *J Bacteriol* **169**: 751–757.
Bradshaw RA, Yi E. (2002). *Essays Biochem* **38**: 65–78.
Catalano A, Romano M, Robuffo I, Strizzi L, Procopio A. (2001). *Am J Pathol* **159**: 721–731.
Chang SY, McGary EC, Chang S. (1989). *J Bacteriol* **171**: 4071–4072.
Chang YH, Teichert U, Smith JA. (1990). *J Biol Chem* **265**: 19892–19897.
Chen S, Vetro JA, Chang YH. (2002). *Arch Biochem Biophys* **398**: 87–93.
Corpet F. (1988). *Nucleic Acids Res* **16**: 10881–10890.
Cutforth T, Gaul U. (1999). *Mech Dev* **82**: 23–28.
Endo H, Takenaga K, Kanno T, Satoh H, Mori S. (2002). *J Biol Chem* **277**: 26396–26402.
Flinta C, Persson B, Jornvall H, von Heijne G. (1986). *Eur J Biochem* **154**: 193–196.
Garrabrant T, Tuman R, Ludovici D, Tominovich R, Simoneaux R, Galemmo R. (2004). *Angiogenesis* **7**: 91–96.
Giglione C, Meinnel T. (2001). *Trends Plant Sci* **6**: 566–572.
Giglione C, Serero A, Pierre M, Boisson B, Meinnel T. (2000). *EMBO J* **19**: 5916–5929.
Giglione C, Vallon O, Meinnel T. (2003). *EMBO J* **22**: 13–23.
Higgins DG, Thompson JD, Gibson TJ. (1996). *Methods Enzymol* **266**: 383–402.
Johnson DR, Bhatnagar RS, Knoll LJ, Gordon JI. (1994). *Annu Rev Biochem* **63**: 869–914.
Kanno T, Endo H, Takeuchi K, Morishita Y, Fukayama M, Mori S. (2002). *Lab Invest* **82**: 893–901.
Kinder Jr FR, Versace RW, Bair KW, Bontempo JM, Cesarz D, Chen S *et al*. (2001). *J Med Chem* **44**: 3692–3699.
Li X, Chang YH. (1995). *Proc Natl Acad Sci USA* **92**: 12357–12361.
Lowther WT, Matthews BW. (2000). *Biochim Biophys Acta* **1477**: 157–167.
Meinnel T, Mechulam Y, Blanquet S. (1993). *Biochimie* **75**: 1061–1075.
Miller CG, Strauch KL, Kukral AM, Miller JL, Wingfield PT, Mazzei GJ *et al*. (1987). *Proc Natl Acad Sci USA* **84**: 2718–2722.
Serero A, Giglione C, Sardini A, Martinez-Sanz J, Meinnel T. (2003). *J Biol Chem* **278**: 52953–52963.
Serero A, Giglione C, Meinnel T. (2001). *J Mol Biol* **314**: 695–708.
Sing N, Meng L, Wang MQ, Wen JJ, Bornmann WG, Crews CM. (1997). *Proc Natl Acad Sci USA* **94**: 6099–6103.
Towbin H, Bair KW, DeCaprio JA, Eck M, Kim S, Kinder FR *et al*. (2003). *J Biol Chem* **278**: 52964–52971.
Varshavsky A. (1996). *Proc Natl Acad Sci USA* **93**: 12142–12149.